# Atomic collision experiment using ultra-slow antiproton beams

**Article** *in* Journal of Physics Conference Series · September 2007

DOI: 10.1088/1742-6596/80/1/012022



**11 authors**, including:

Daniel Barna
Wigner Research Centre for Physics, Budapest
**152** PUBLICATIONS **4,201** CITATIONS
SEE PROFILE

Victor Varentsov
Facility for Antiproton and Ion Research in E…
**73** PUBLICATIONS **433** CITATIONS
SEE PROFILE

Yasunori Yamazaki
RIKEN
**390** PUBLICATIONS **4,765** CITATIONS
SEE PROFILE

Journal of Physics: Conference Series **80** (2007) 012022 doi:10.1088/1742-6596/80/1/012022

# Atomic collision experiment using ultra-slow antiproton beams

**Hiroyuki A Torii[1], N Kuroda[2], M Shibata[2], H Imao[2], Y Nagata[1,2], D Barna[3], M Hori[3], Y Kanai[2], A Mohri[2], V L Varentsov[4] and Y Yamazaki[1,2]**

[1] Institute of Physics, University of Tokyo, 3-8-1 Komaba, Meguro-ku, Tokyo 153-8902, Japan
[2] Atomic Lab., RIKEN, 2-1 Hirosawa, Wako-shi, Saitama 351-0198, Japan
[3] CERN, Genève 23, CH-1211, Switzerland
[4] V G Khlopin Radium Institute, 2-nd Murinsky Ave. 28, 194021 St. Petersburg, Russia

E-mail: torii@radphys4.c.u-tokyo.ac.jp

**Abstract.** The development of techniques to decelerate, cool and confine antiprotons in vacuo with an electromagnetic trap has opened a new research field of atomic physics of 'cold' antiprotons, including synthesis of antihydrogen atoms. At the Antiproton Decelerator (AD) facility at CERN, we the MUSASHI group of ASACUSA collaboration have so far achieved efficient confinement of millions of antiprotons in a Multi-Ring electrode Trap (MRT) installed in a superconducting magnet of 2.5 T, by a sequential combination of the AD (down to 5.3 MeV), an RFQD (Radio-Frequency Quadrupole Decelerator; down to 50–120 keV) and the MRT. Antiprotons, cooled to energies less than an electronvolt by preloaded electrons in the trap, was then extracted out of the magnetic field and transported along a 3-m beamline as a monoenergetic beam of 10–500 eV. With this unique ultra-low-energy antiproton beam, we are now planning the first atomic collision experiments under single collision conditions, to measure ionization and atomic capture cross sections of antiprotons against helium atoms. A supersonic atomic gas-jet target is prepared and crossed with the antiproton beam. Antiprotons as well as electrons emitted during the reaction will be detected by a microchannel plate (MCP) while the antiproton annihilation will be recognized by detection of annihilation products — mostly pions — by surrounding scintillation counters. When the antiproton is captured, it forms a neutral antiprotonic helium atom, some in a metastable state whose level structures have been well studied with spectroscopic methods. Severe identification of particles and atoms plays an essential role in the design of the experiment, to distinguish the small number of reaction events out of a huge pile of background events. Our strategies for our near-future experiments are discussed.

## 1. Introduction

Antiproton, the antiparticle of proton, would be an interesting new probe for atomic physics researches, if it can be prepared either at rest or as a beam with a typical "atomic energy" in the eV to keV range. Having the same mass as the proton but with opposite charge, It behaves as a "heavy electron" or as a "negative nucleus", and gives a new test ground for studies of atomic collision dynamics. In fact, it is a "theoreticians' ideal projectile" because lack of electron capture processes avoids complication in theoretical treatments.

Experimentally, antiprotons can be produced at accelerator facilities, but only at a huge energy in the GeV range. The Antiproton Decelerator (AD) [1] at CERN, Geneva, is a unique

facility which provides cooled low-energy antiprotons with MeV energies. There, the ASACUSA collaboration has been doing researches on "Atomic Spectroscopy And Collisions Using Slow Antiprotons" [2].

One branch of our activities is the spectroscopy of metastable antiprotonic helium atom [3]. This three-body atom consisting of a helium nucleus, an electron and an antiproton is a peculiar system, which can be regarded as a mixture of matter and antimatter, and yet shows longevity of a few microseconds at large quantum numbers of $n \sim 38$ and $l \lesssim n$. Laser and microwave spectroscopy has not only revealed the level structure of this exotic atom [4, 5], but also assisted development of calculation techniques for the Coulombic three-body system, in the precision competition between the experiment and the theory [6]. Recent high precision in our laser spectroscopy has reached the level of $10^{-9}$ in determination of transition frequencies, and comparison with the theoretical QED calculations now gives one of the most precise values for the antiproton-to-electron mass ratio as well as the antiproton-to-proton mass ratio [7], contributing to the precise determination of the fundamental constant and to the test of CPT invariance theorem.

Another branch of our research deals with atomic collision dynamics involving low-energy antiprotons. In the experimental realization, an ultra-slow antiproton beam at a well-defined energy in the eV to keV range must be prepared for antiproton–atom cross-beam experiment. We the MUSASHI group the ASACUSA collaboration developed a system consisting of an RFQ Decelerator, an electromagnetic trap and an extraction beamline, and have recently succeeded in production of ultra-low-energy monoenergetic antiproton beams. These beams are crossed with an atomic gas-jet target, to study ionization and atomic capture processes of an antiproton projectile against various atoms "A",

$$\overline{p} + \mathrm{A} \rightarrow \overline{p} + \mathrm{A}^{+} + e^{-}$$

$$\overline{p} + \mathrm{A} \rightarrow (\overline{p}\mathrm{A}^{+})^{0} + e^{-}$$

for the first time under single-collision condition at very low energies.

## 2. Deceleration of antiproton beam

At CERN, antiprotons are produced by collision of protons at 26 GeV/$c$ with an Ir target via the reaction $p + p \rightarrow p + p + p + \overline{p}$. A part of them, $5 \times 10^7$ in number, are collected at 3.6 GeV/$c$ and stored in the AD ring [1], which are then cooled via electron cooling and stochastic cooling techniques [8, 9] and decelerated down to a momentum of 100 MeV/$c$ or 5.3 MeV in kinetic energy, before they are extracted to experimental zones as a pulsed beam of typically $3 \times 10^7$ antiprotons in a bunch of 100–200 ns (see Fig. 1).

Thus produced antiproton beam, though already lower in energy by 3 orders of magnitude than at production, needs further deceleration for them to be captured in vacuo electrostatically. In order to decelerate antiprotons efficiently, the ASACUSA collaboration [2] developed a Radio Frequency Quadrupole Decelerator (RFQD) [10] in collaboration with the CERN PS group. An RF wave was applied to the cavities in such a way as to decelerate microbunches of the antiproton beam at 5.3 MeV down to 63 keV with an efficiency of 30%. Since the RF cavities can be biased ± 60 keV, the output antiproton energy can be varied 10–120 keV.

The output beam from the RFQD was injected into an eletromagnetic trap in a strong magnetic field of 2.5 T produced by a superconducting solenoid. The beam was focused to a diameter of 3–4 mm on a thin Mylar i.e. PET (polyethylene terephthalate) double-layered foil of 90 $\mu$g/cm$^2$ for each layer [11], used to isolate ultrahigh vacuum of $10^{-12}$ mbar inside the trap.

Taking into account the energy loss in the foil, we set the bias voltage of the RFQD to 110 kV so as to maximize the number of antiprotons captured, with their transverse energy less than 10 keV after penetration through the foil.

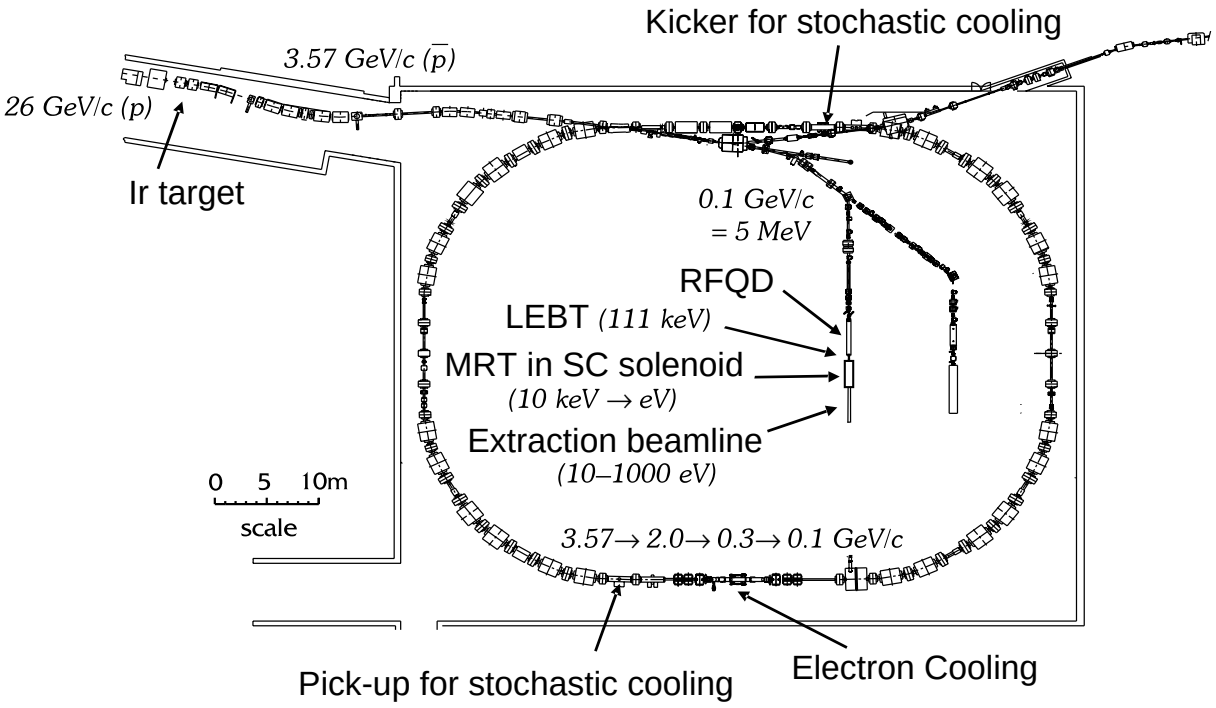


**Figure 1.** Layout of the Antiproton Decelerator (AD) at CERN.

## 3. Confinement and cooling

Antiprotons were then captured and confined in the trap. We used a Multi-Ring Trap (MRT) [12] consisting of 14 cylindrical electrodes placed coaxially along the magnetic field line. A favorable feature of the MRT compared with a normal Penning trap and a trap with a well-type potential is that a harmonic electric potential can be prepared in a wide region near the trap axis by application of appropriate voltage on each electrode, which enables extremely stable confinement of a large number of charged particles.

Figure 2 shows sequential steps for antiproton capture, cooling and extraction. The pulse of incident antiprotons were reflected backward at the DCE electrode floated at $-10$ kV. By the time the pulse returned after its round trip of typically 500 ns back to the UCE, the trap was closed by a fast switch which biased the UCE to $-10$ kV, confining a major part of the antiprotons. The antiprotons were then cooled by a plasma of typically $3 \times 10^8$ electrons preloaded in the harmonic potential. Antiprotons lost their energy by transferring it to electrons, while the heated electrons cooled by themselves by emission of synchrotron radiation in the magnetic field of 2.5 T, until the antiprotons were trapped in the bottom of the harmonic potential of 50 V depth. We then opened one side of the potential for 550 ns to selectively release electrons: lighter and thus faster electrons escaped within this short period, while heavier and much slower antiprotons remained inside. This release of electron was necessary for efficient extraction of antiprotons. The antiproton cloud was then given torque by a rotating electric field to be compressed radially. For this purpose, one of the electrodes was segmented azimuthally into four parts, and an RF voltage was applied to each segment with a phase difference of $\pi/2$ next to each other [13].

In order to diagnose cooling process of the antiproton in the trap, we prepared a set of track detectors to know the position and time of antiproton annihilation (see Fig. 3). Two scintillator bars of 2 m in length, with a rectangular cross section of 4(H) $\times$ 6(V) cm$^2$, were placed in the same plane and parallel to the trap axis. Passage of charged particles such as pions, or

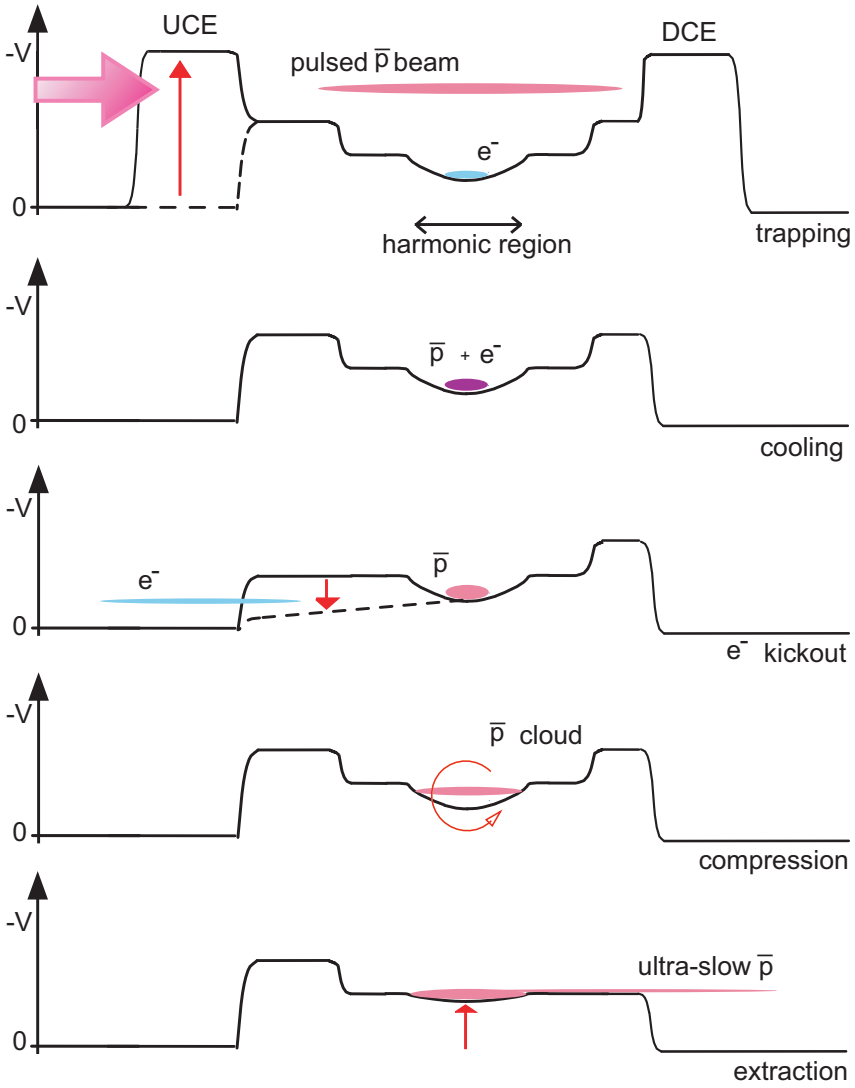


**Figure 2.** Sequential procedures of antiproton capture, cooling and extraction.

electron-positron showers converted from gamma rays originating in the decay of neutral pions, was detected and the position of the crossing points calculated from the time-of-flight difference of the scintillation light arriving at photomultiplier tubes (PMTs) at both ends of the bars. Tracking back the reconstructed particle trajectory onto the trap axis, antiproton annihilation can be detected with a position resolution of 20 cm and with a detection efficiency of $\epsilon \sim 5\%$, which agreed with our simulation using GEANT trajectory calculation code [14]. Figure 4 shows detected annihilation counts as a function of time and position along the beam axis (i.e. the trap axis). Frequent annihilation was observed at early times for a typical period of 10 s following antiproton injection at $t = 0$. They occurred at positions of the degrader foil and the trap. After the antiprotons have been cooled enough, there still remained constant annihilation in the trap center when the temperature of the bore which housed the trap electrodes was 25 K. This was due to continuous antiproton annihilation against atomic nuclei of residual gases, mainly hydrogen. A standard "ultra-high" vacuum is not apparently good enough for stable confinement of antiprotons. On the other hand, no annihilation was observed during confinement

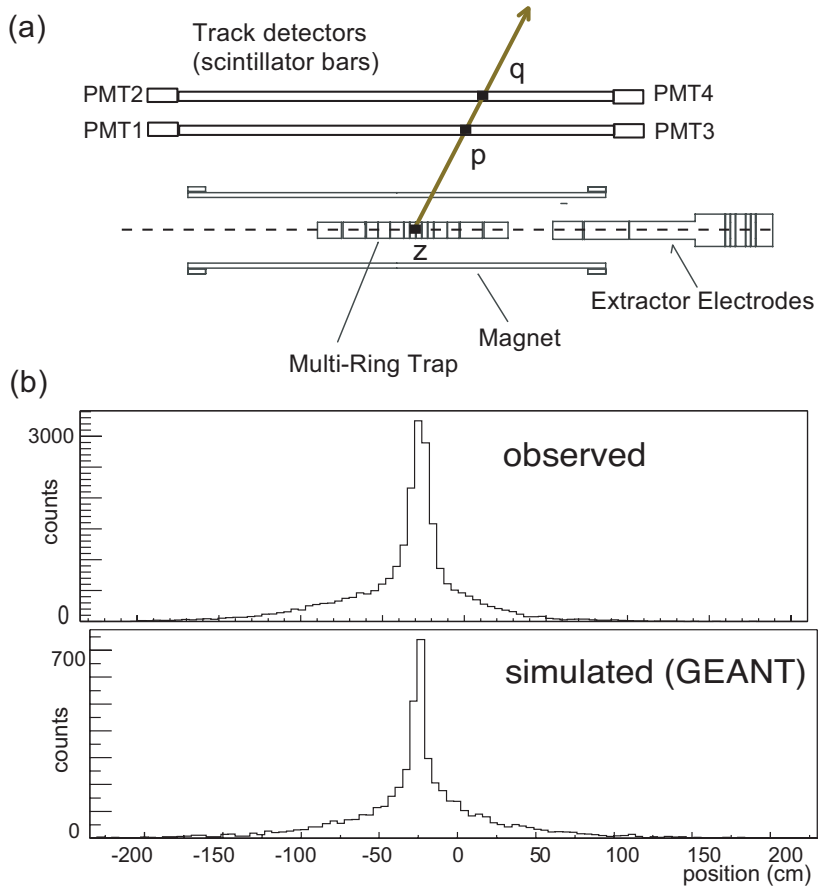


**Figure 3.** Position of antiproton annihilation can be calculated from the trajectory of produced particles, detected by scintillator bars. Observed position resolution agreed with our simulation using GEANT code.

at the bore temperature of 7 K. At this cryogenic temperature, even the hydrogen gas freezed out and an extremely high vacuum better than $10^{-12}$ mbar was achieved, preventing antiproton annihilation. Antiprotons were then extracted and annihilation peaks were seen at downstream of the MRT.

Integrating the number of antiproton annihilations over all the positions, we obtain the total number of trapped antiprotons. With this trap, we successfully confined $1.2 \times 10^6$ cooled antiprotons until the end of our trap cycle of 1–5 minutes [15]. Typically 1 million antiprotons were trapped for each AD shot. We then accumulated antiprotons for several AD shots. This technique of "stacking" also worked fine, and we trapped $4.8 \times 10^6$ antiprotons simultaneously for stacking of 5 AD shots, the largest number of antiprotons ever accumulated.

## 4. Extraction and beam transport

The antiprotons were then released from the trapping potential as it was gradually shallowed, and were extracted as an ultra-slow continuous beam of 10–500 eV. Since the antiprotons tend to expand in radial direction when they follow the strongly diverging magnetic field line, it was essential that the antiproton cloud be well compressed radially in the trap [13]. Precise alignment of the magnetic field axis, electric trap axis, and the beam transport axes was also important in efficient extraction; a misalignment of even a few milliradians was enough to prevent effective

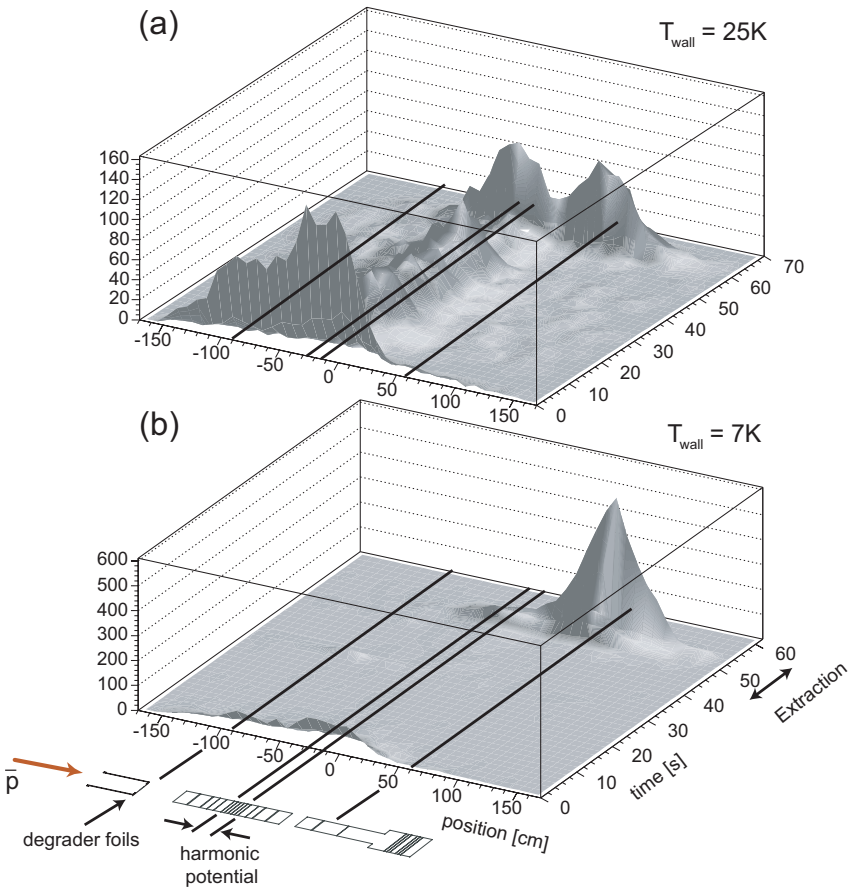


**Figure 4.** Antiproton annihilation observed by the track detectors are counted as a function of time and position. The temperature of the bore tube was (a) 25 K and (b) 7 K. Continuous antiproton annihilation in the trap at 25 K is attributed to antiprotons colliding against residual gas, indicating that an extremely high vacuum of $10^{-12}$ mbar realized at 7 K is needed for stable antiproton storage.

extraction.

The extraction beamline was designed to transport antiproton beams over a length of 3 m, at variable energies ranging from 10 to 1000 eV. The antiproton beams were refocused three times by sets of Einzel lenses at the position of apertures, as shown in Fig. 5. These variable apertures of diameter 4–10 mm allow differential pumping of 6 orders of magnitude along the beamline [16], which was necessary to keep the trap region at an extremely high vacuum better than $10^{-12}$ mbar so as to avoid antiproton annihilation, while the end of the beamline is to be exposed to atomic or molecular gas jets of upto $10^{-6}$ mbar.

The MRT, the superconducting solenoid and the transport line for the ultra-slow beam are jointly known as "MUSASHI", or the Monoenergetic Ultra-Slow Antiproton Source for High-precision Investigations. MUSASHI opens a new research field ranging from atomic physics to nuclear physics [17, 18, 19, 20], including our near-future project of antihydrogen synthesis in a cusp trap [21].

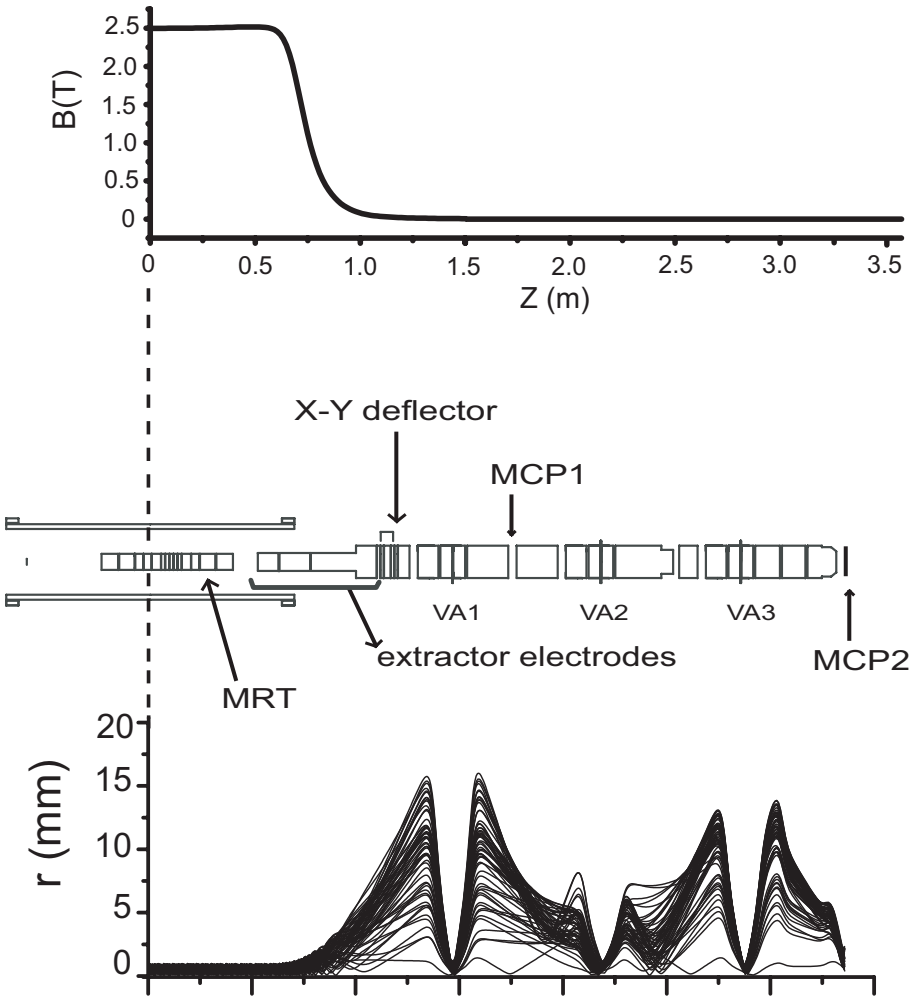


**Figure 5.** Schematic of the extraction beamline for ultra-slow antiproton beams. The beams are focused 3 times at positions of variable apertures (VAs), to comply with the requirement of effective differential pumping (bottom). Magnetic field strength is also shown in the top figure.

## 5. Atomic collision experiments

With this unique beam, atomic formation and ionization processes by very-low-energy antiprotons can now be studied under single collision conditions for the first time.

Since the number of available antiprotons is very much limited, the reaction probability must be maximized in order to make best use of them, and therefore a maximum possible density of the atomic gas jets need to be prepared to be crossed with the antiproton beams. Then the number of antiprotonic atoms formed is given by the formula

$$N_{\overline{p}\mathrm{A}^+} = \sigma \, n_\mathrm{A} \, L \, N_{\overline{p}} \, ,$$

where $\sigma$ is the formation cross section, $n_\mathrm{A}$ the number density of the atomic target, $L$ the interaction length, and $N_{\overline{p}}$ is the number of antiprotons.

Atomic formation cross sections are naturally of the order of $10^{-16}$ cm$^2$ [22]. Suppose a beam with $10^5$ antiprotons is available every shot per several minutes, we will obtain $10^2$ antiprotonic atoms for a gas density of $10^{13}$ atoms/cm$^3$ at an interaction length of 1 cm. The reaction probability is of the order of 0.1%. This number is almost at the lower limit of detection in

order to assure enough statistical significance for the formation events to be distinguished from background events.

## 6. Gas-jet target

At our early stage of development, several ideas for realization of the gas target was considered [23]. Usage of effusive gas out of micro-capillary array was also considered, but was rejected in favor of supersonic gas targets for two main reasons: 1) the gas jet should be well-collimated and 2) the background vacuum should be kept at a level below $10^{-6}$ mbar.

Helium atom was chosen for our first target, for technical simplicity and because of the fact that the lifetime of antiprotonic helium atoms are already known from our spectroscopic measurements [24]. Atomic and molecular hydrogen targets are also interesting and simple from theoretical point of view, but we shall consider them later in our next step, because preparation of these hydrogen targets confront experimental difficulties including special safety precautions.

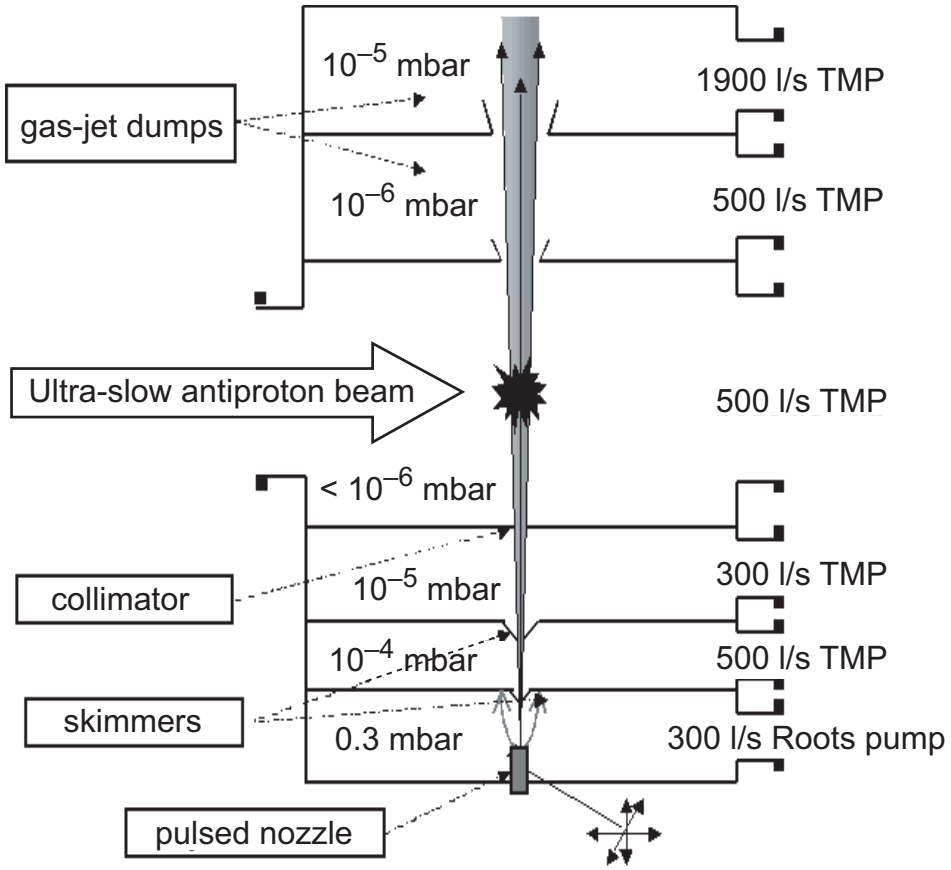


**Figure 6.** Schematic design of our supersonic gas-jet system.

Figure 6 shows a schematic design of our apparatus for the supersonic gas-jet target [25]. It has 6 chamber stages in order to achieve good beam collimation and efficient pumping. A supersonic gas jet emerging from a 0.1-mm-diameter nozzle was skimmed by two stages of conically shaped skimmers with a hole diameter of 0.6 mm and 2.2 mm. The stagnation pressure before the nozzle was optimized at 25 bar at room temperature, for production of a powerful jet with a large Mach number of 35.8 according to our gas-jet flow simulation. A Pitot tube was used in advance to monitor the pressure profile of the gas jet, in order to determine the optimum distance between the nozzle and the first skimmer.

Most of the gas out of the nozzle was skimmed away and was differentially pumped. A powerful 300 l/s Roots pump was employed to cope with the great gas load at 0.3 mbar at the first stage, while the other chamber stages with better vacuum than $10^{-4}$ mbar were pumped by turbo-molecular pumps (TMPs) with a large pumping speed of typically 500 l/s. The gas jet was then collimated to form a target of 1 cm diameter at the cross point in the main chamber. The jet was then collected at the dump stages with an over-90% efficiency by powerful TMPs (the main one having a pumping speed of 1900 l/s). The vacuum in the main chamber was kept to a level of less than $10^{-6}$ mbar.

The nozzle had a poppet valve just in front of it, operated by a small solenoidal magnet. Open and close of the gas-jet flow can be controlled by an external electric switch, and the equilibrium of the gas flow was reached within a small fraction of a second after the switch was turned on. This pulsed valve allows economical usage of the gas jet which is turned on only during the extraction period of the antiproton beam in a whole cycle of antiproton capture, cooling, trapping and extraction, and hence reduction of the total gas load.

## 7. Antiproton beam trajectory

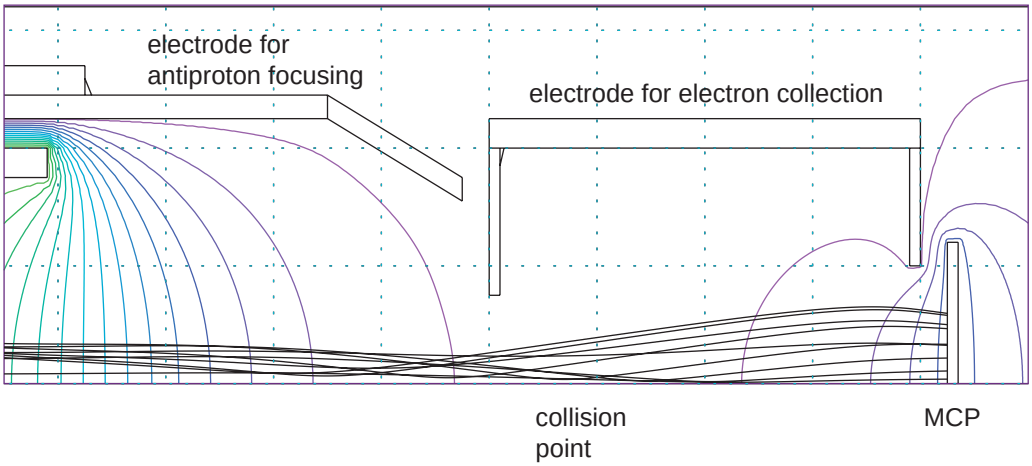


**Figure 7.** Simulated antiproton trajectoris at 250 eV at the last stage of the beamline. The antiproton is well focused near the cross point to overlap the gas-jet target while the beam divergence is kept small enough for the beam to be detected within the sensitive area with a 4-cm diameter of the MCP placed 6.5 cm downstream.

Designing the beam transport of ultra-slow antiprotons is not a trivial task at this very low energy. The antiproton beam needs to go through 3 aperture stages along the 3-m extraction beamline before it is focused at the collision point [16]. The last focusing has to fulfill two contradictory conditions: the beam spot must be squeezed to the small size of the gas jet, yet the focusing has to be weak enough to keep the beam divergence to a small value so that all the antiprotons and antiprotonic atoms should be collected at the sensitive area of an MCP downstream. Figure 7 shows a solution to the simulation of antiproton trajectories at 250 eV, from the last stage of our beamline through the collision point against the gas-jet target, until the MCP downstream. The MCP is biased at +470 eV to draw in the negative particles. The beam size is squeezed to a diameter of 8 mm at the waist, to ensure a good overlap with the gas jet.

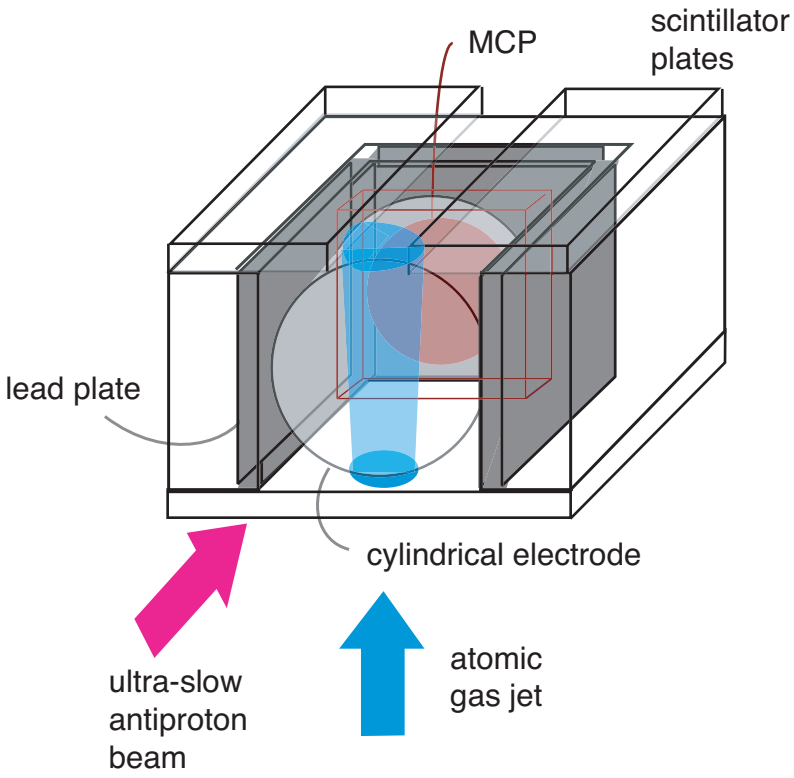


**Figure 8.** Schematic setup of detectors surrounding the collision point of the antiproton beam and the gas-jet target.

## 8. Detection and data acquisition systems

Antiprotons are extracted as a beam in a slow-extraction mode. This continuous beam allows event-by-event data acquisition associated with each single antiproton extracted. For particle detection, the microchannel plate (MCP) with a two-demensional position sensitive detector is placed 6.5 cm downstream of the antiproton beam from the cross point, and is surrounded by a box of lead plates and scintillator plates (see Fig. 8). The above-mentioned good vacuum level in the main chamber is required also for proper operation of the MCP without a risk of discharge. An antiproton impacts a helium atom and ionizes it, emitting an electron, which is then guided by a cylindrical electrode toward the MCP with an efficiency larger than 90%. Depending on the impact energy, the antiproton either travels downstream at a lower energy or is captured to form an antiprotonic helium atom which flies at an even lower speed toward downstream. The MCP is used to detect any of these particles: an electron, a bare antiproton, or an antiprotonic atom; while the scintillation counter detects passage of high-energy particles such as pions, originating from antiproton annihilation.

The key point in this experiment is the rigorous identification of particles. As was mentioned above, the reaction probability is about 0.1%. So that one single proper reaction event must be well identified out of the rest 999 antiproton annihilation events without reaction. The solid angle coverage of the scintillation counter is nearly 90% seen from the MCP. Antiproton annihilation is usually accompanied by emission of 3 charged pions on average and 2 neutral pions. A neutral pion decays into 2 gamma rays, which are converted to electromagnetic showers of electrons and positrons in the lead plates, and together with charged pions, they can be detected by the scintillation counter. This multiplicity of the annihilation products helps to achieve an extremely high detection efficiency of 99.7% for the detection of antiproton annihilation [26]. Thus, an

electron signal is identified by an MCP hit and no scintillator hit, while an antiproton signal is identified by the coincidence of both MCP and scintillator hits. The signals are processed and recorded by standard NIM and CAMAC systems and a set of computers (as they are often used in high-energy experiments). The reaction event is then recognized in the analysis program by an electron signal followed by an antiproton signal with an appropriate TOF (time-of-flight) interval, mainly determined by the TOF of the slower antiproton or the antiprotonic atom.

## 9. Future scope

After a recent test experiment with promising results on the check of the detection schemes using the antiproton beam, we are now ready for our coming beam experiments to measure the reaction cross sections in the energy range of 10 eV to 500 eV using the above-described apparatus.

As for ionization of atoms by antiproton at higher energies, the cross sections were measured in the 1990s using degraded direct beam from the LEAR (Low-Energy Antiproton Ring) facility, the predecessor of AD. The experimental results taken in a wide range between 10 keV to 3 MeV illustrated an interesting curve [27, 28], which agreed with most of theoretical calculations except for the energies less than 30 keV. This discrepancy remained a puzzle until recently.

The ultra-slow MUSASHI antiproton beam can also be used for experiments at energies in the 1–20 keV range, if the beam is re-accelerated toward a target in an electrically floated apparatus. Using this method, we together with a group from Aarhus University in the ASACUSA collaboration have recently measured ionization cross section of helium atoms by antiproton impact at energies in the 5–20 keV range. The detail of this measurements and our successful results which now seem to agree with theoretical calculations, shall be explained in our future publication.

One of the important topics related with low-energy antiproton is antihydrogen. Following the first production of antihydrogen in 1995 in the LEAR ring [29], two collaborations ATHENA (now named ALPHA) and ATRAP at AD succeeded in synthesis of cold antihydrogen atoms out of antiprotons and positrons confined in a nested Penning trap, and are pursuing their goal of spectroscopy of the anti-atom [30, 31]. We the ASACUSA collaboration is also preparing for antihydrogen synthesis using two different approaches, one with a cusp trap and another with a Paul trap. The cusp trap employs an anti-helmholtz coil to create a magnetic quadrupole field and a multi-ring trap (MRT) to generate various electric fields such as an octupole field [21]. A great feature of this trap is that it can confine both antiproton and positron at the same time, and also neutral antihydrogen atoms as well. Antihydrogen atoms in the low-field-seeking high-Rydberg states are confined by the magnetic field gradient, and they are then cooled [32] and cascade down to the $1S$ ground state. These antihydrogen atoms are expected to escape from the trap to form a spin-polarized beam, and then a microwave spin-flip experiment may be possible to measure precisely the antiproton's magnetic moment, which is currently known only to a level of $10^{-3}$.

## Summary

We have succeeded in deceleration, cooling and confinement of a large number of antiprotons provided at the AD facility at CERN, using a combination of the RFQ Decelerator and the multi-ring electrode trap. The antiprotons were then extracted out of the strong magnetic field to form an ultra-slow antiproton beam in the energy range of 10–500 eV. This unique beam opens a new research field of atomic physics including antihydrogen synthesis. Especially, the cross-beam experiment against our supersonic gas-jet target will reveal the ionization and atomic capture processes involving antiproton projectile.

**Acknowledgments**
We are grateful to the AD and PS stuff in the AB department of CERN for their tireless effort in providing us with the antiproton beam. We acknowledge Mr. W. Pirkl and his team for their engagement in the design and operation of the RFQD. This work was supported by the Grant-in-Aid for Creative Scientific Research (10P0101) of the Japanese Ministry of Education, Culture, Sports, Science and Technology (MonbuKagaku-shō), Special Research Projects for Basic Science of RIKEN, and the Hungarian National Science Foundation (OTKA T033079).

## References

[1] CERN Antiproton Decelerator web page, `http://psdoc.web.cern.ch/PSdoc/acc/ad/index.html`
[2] ASACUSA collaboration web page, `http://cern.ch/ASACUSA`
[3] Yamazaki T *et al* 2002 *Phys. Rep.* **366** 183
[4] Morita N *et al* 1994 *Phys. Rev. Lett.* **72** 1180
[5] Widmann E *et al* 2002 *Phys. Rev. Lett.* **89** 243402
[6] Torii H A *et al* 1999 *Phys. Rev.* A **59** 223
[7] Hori M, Dax A *et al* 2006 *Phys. Rev. Lett.* **96** 243401
[8] Budker G I and Skrinski A N 1978 *Sov. Phys. Usp.* **21** 277
[9] van der Meer S 1981 *IEEE Trans. Nucl. Sci.* **NS28** 1994
[10] Lombardi A M, Pirkl W, and Bylinsky Y 2001 *Proceedings of the 2001 Particle Accelerator Conference, Chicago (IEEE, Piscataway, NJ)* 585
[11] Hori M, private communication. cf. also 2004 *Nucl. Insturm. Methods.* A **522** 420
[12] Mohri A, Higaki H *et al* 1998 *Jpn. J. Appl. Phys.* **37** 664
[13] Kuroda N *et al to be published.*
[14] GEANT3, CERN Program Library Long Writeup W5013
[15] Kuroda N, Torii H A, Yoshiki Franzen K, Wang Z, Yoneda S, Inoue M, Hori M, Juhász B, Horváth D, Higaki H, Mohri A, Eades J, Komaki K, and Yamazaki Y 2005 *Phys. Rev. Lett.* **94** 023401
[16] Yoshiki Franzen K, Kuroda N, Torii H A, Hori M, Wang Z, Higaki H, Yoneda S, Juhász B, Horváth D, Mohri A, Komaki K and Yamazaki Y 2003 *Rev. Sci. Instrum.* **74** 3305
[17] Yamazaki Y, 1999 *Nucl. Instrum. Methods in Phys. Res.* B **154** 174
[18] Trzcińska A *et al* 2001 *Phys. Rev. Lett.* **87** 82501
[19] Jastrzębski *et al* 1993 *Nucl. Phys.* A **558** 405c
[20] Wada M and Yamazaki Y 2004 *Nucl. Instrum. Methods in Phys. Res.* B **214** 196
[21] Mohri A and Yamazaki Y 2003 *Europhys. Lett.* **63** 207
[22] Cohen J S 2004 *Rep. Prog. Phys.* **67** 1769; Cohen J S 2005 *AIP Conf. Proc.* **793** 98
[23] Wang Z 2002 *internal report, unpublished*
[24] Hori M *et al* 2004 *Phys. Rev.* A **70** 012504
[25] Varentsov V L, Kuroda N, Nagata Y, Torii H A, Shibata M, Yamazaki Y 2005 *AIP Conf. Proc.* **793** 328
[26] Torii H A *et al* 1997 *Nucl. Instrum. Methods in Phys. Res.* A **396** 257
[27] Anderson L H *et al* 1990 *Phys. Rev.* A **41** 6536
[28] Hvelplund P *et al* 1997 *J. Phys.* B **27** 925
[29] Baur G *et al* 1996 *Phys. Lett.* B **368** 251
[30] Amoretti M *et al* 2002 *Nature* **419** 456
[31] Gabrielse G *et al* 2002 *Phys. Rev. Lett.* **89** 213401
[32] Pohl T, Sadeghpour H R, Nagata Y, and Yamazaki Y 2006 *Phys. Rev. Lett.* **97** 213001